HHS Public Access

Author manuscript

Immunity. Author manuscript; available in PMC 2017 November 19.

Published in final edited form as:

Immunity. 2016 November 15; 45(5): 975–987. doi:10.1016/j.immuni.2016.10.011.

Deleting an *Nr4a1* super-enhancer subdomain ablates Ly6C^{low} monocytes while preserving macrophage gene function

Graham D. Thomas[1], **Richard N. Hanna**[1], **Neelakatan T. Vasudevan**[2], **Anouk A. Hamers**[1], **Casey E. Romanoski**[3], **Sara McArdale**[1], **Kevin Ross**[4], **Amy Blatchley**[1], **Debbi Yoakum**[1], **Bruce A. Hamilton**[4], **Zbigniew Mikulski**[1], **Mukesh K. Jain**[2], **Christopher K. Glass**[4], and **Catherine C. Hedrick**[1,5]

[1]Division of Inflammation Biology, La Jolla Institute for Allergy and Immunology, La Jolla, CA 92037, USA

[2]Case Cardiovascular Research Institute, Department of Medicine, Harrington Heart and Vascular Institute, University Hospitals Case Medical Center, Cleveland, OH 44106, USA

[3]Keating Bioresearch Building, 1657 E. Helen St, Tucson, AZ 85721, USA

[4]Department of Cellular and Molecular Medicine, University of California, San Diego, 9500 Gilman Drive, La Jolla, CA 92093, USA

Summary

Mononuclear phagocytes are a heterogeneous family that occupy all tissues and assume numerous roles to support tissue function and systemic homeostasis. Our ability to dissect the roles of individual subsets is limited by a lack of technologies that ablate gene function within specific mononuclear phagocyte sub-populations. Using *Nr4a1*-dependent Ly6C^{low} monocytes we present a proof-of-principle approach that addresses these limitations. Combining ChIP-Seq and molecular approaches we identified a single, conserved, sub-domain within the *Nr4a1* enhancer that was essential for Ly6C^{low} monocyte development. Mice lacking this enhancer lacked Ly6C^{low} monocytes but retained *Nr4a1* gene expression in macrophages during steady state and in response to LPS. As *Nr4a1* regulates inflammatory gene expression and differentiation of Ly6C^{low} monocytes, decoupling these processes allows Ly6C^{low} monocytes to be studied independently.

Graphical abstract

[5]Lead Contact. hedrick@lji.org

Accession Numbers

Illumina sequencing for this project have been deposited at NCBI's Gene Expression Omnibus (GEO) as a SuperSeries under the accession number GSE80040.

Author contributions

Conceptualization CCH, CKG and GDT; Methodology GDT, RNH, CER, KDR, BAH; Software, formal analysis and visualization GDT; Investigation GDT, AB and DY; Resources MKJ, VNT, ZM and SM; Writing - original draft GDT and CCH; Writing - Reviewing and Editing - all authors; Funding Acquisition CCH and GDT.

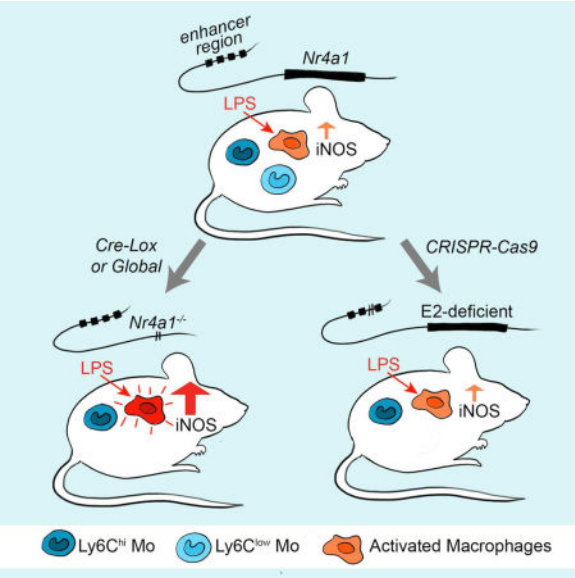

Introduction

Mononuclear phagocytes (MP) are an ontologically diverse family of cells comprised of macrophages and monocytes (Perdiguero and Geissmann, 2016). From a traditional standpoint the primary functions of MP involve recognition and clearance of invading pathogens, maintaining tissue integrity and resolving inflammation (Sica and Mantovani, 2012). To perform these diverse functions MP occupy all bodily tissues and display a tremendous degree of phenotypic plasticity. In recent years transcriptomic profiling efforts have revealed the full extent of this heterogeneity, and functional studies have unveiled diverse, specialized and often unexpected roles for individual MP subsets (Amit et al., 2016). In this context, tissue macrophages and blood monocytes may be considered accessory cells that allow optimal performance of the host tissue (Okabe and Medzhitov, 2016). In complement to their roles in immunity and host defense, tissue MP are now also recognized as major regulators of higher-order physiological processes including systemic energy balance (Odegaard and Chawla, 2011), intestinal peristalsis (Muller et al., 2014) and cognitive function (Parkhurst et al., 2013). Delineating the full extent of MP functions in health and disease represents a largely unexplored frontier in both immunology and physiology.

Monocytes constitute the blood-borne phase of the MP system and are composed of at least two subsets in both mouse and human that are believed to be conserved (Cros et al., 2010). Mouse monocyte subsets can be discriminated using the Ly6C surface antigen (Geissmann et al., 2010), Ly6C^{hi} monocytes are progenitors of inflammatory, and some tissue-resident macrophages. Ly6C^{low} monocytes exhibit a patrolling behavior on the vascular endothelium and contribute to vascular homeostasis by maintaining the endothelial layer (Carlin et al., 2013). In addition, Ly6C^{low} monocytes have recently been shown to play a crucial role protecting against the seeding of tumor metastases in the lung (Hanna et al., 2015).

An indispensable approach to understand cellular behavior is through loss-of-function. The identification of lineage defining transcription factors (LDTFs) for MP subsets has led to new insights into the functions of these cells. For example, the transcription factor *Nr4a1* is the master regulator of the Ly6C^{low} monocyte subset (Hanna et al., 2011). *Nr4a1* is uniquely highly expressed in Ly6C^{low} monocytes, and is required in a cell-intrinsic fashion. Accordingly *Nr4a1*$^{-/-}$ mice were instrumental in revealing a role for Ly6C^{low} monocytes in tumor metastasis (Hanna et al., 2015). In another example, loss of the transcription factor *Spic* selectively ablates splenic red pulp macrophages revealing a role for this population in iron homeostasis (Kohyama et al., 2009). Similarly macrophage-specific deletion of *Gata6* impairs the maturation of peritoneal macrophages leading to the discovery that these cells modulate B-1 cell IgA production (Okabe and Medzhitov, 2014).

Pleiotropy, exemplified by the differential action of a single gene in multiple cell types, is a major obstacle to understanding cell-specific gene function. To overcome this problem the Cre recombinase-loxP (Cre-Lox) system is routinely used to ablate genes containing loxP-flanked exons by controlling Cre enzyme expression with cell-specific promoters. The ability of the Cre-Lox system to excise gene expression in a cell-specific manner is limited by the cell-specificity of Cre transgenes and the time taken for recombination to occur (Yona et al., 2012). These considerations present problems when using the Cre-Lox system to study gene function within populations of closely related cells. A prime example of this problem is *Nr4a1*. *Nr4a1*$^{-/-}$ mice lack Ly6C^{low} monocytes, macrophage *Nr4a1* is also induced by LPS and represses inflammatory gene expression (Hanna et al., 2012). These confounding influences limit the utility of *Nr4a1*$^{-/-}$ to study Ly6C^{low} monocytes. Furthermore, the current MP Cre transgenes (*Lyz2-cre*, *Csf1r-cre*, *Cx3cr1-cre*) cannot delete Ly6C^{low} monocyte *Nr4a1* without also disrupting *Nr4a1* across MP subsets. These pan-myeloid effects of the current myeloid Cre transgenes limit the ability of conditional deletion approaches to determine gene- and cell-type function within the diverse MP compartment.

Enhancers are genomic sequences that positively influence promoter activity and are critical determinants of signal-dependent and cell-specific gene expression (Andersson et al., 2014). While such elements are rigorously defined by deletion or mutation, they are associated with a distinct chromatin signature that includes enrichment of histone H3 lysine 4 monomethylation (H3K4me1) and (H3K4me2) (Heintzman et al., 2007; Heinz et al., 2010). MP enhancers are enriched for the LDTFs PU.1 and C/EBPβ, which instruct enhancer selection (Heinz et al., 2010). Enhancers are subject to additional regulation leading to their further classification as ‘poised’ or ‘active’. Enhancers are activated upon binding of signal dependent transcription factors (SDTFs), leading to acetylation at H3 lysine 27 (H3K27ac) and the increased expression of associated genes (Creyghton et al., 2010; Heinz et al., 2013). These chromatin features can be used to map enhancer-like regions on a genome-wide scale through the use of ChIP-sequencing. The enhancer landscapes between MP subsets show considerable diversity (Gosselin et al., 2014; Lavin et al., 2014) and result from the myriad environmental niches these populations are exposed to. As *Nr4a1* shows unique expression characteristics in Ly6C^{low} monocytes, we hypothesized a SDTF acting at a cell-specific enhancer regulates transcription of the Ly6C^{low} monocyte LDTF *Nr4a1*.

Here we explore this hypothesis by mapping the *Nr4a1* enhancer locus in Ly6C^{low} monocytes. We identified a single sub-domain 4kb upstream of the *Nr4a1* transcription start site that was essential for Ly6C^{low} monocyte development. Dissection of this element provided insight into the transcriptional processes driving Ly6C^{low} monocyte development. Furthermore, using mice that lack this enhancer we have shown that macrophage *Nr4a1* gene expression was unaffected both in response to inflammatory signaling and during steady state.

Results

Ly6C^{low} monocytes are ontological neighbors to Ly6C^{hi} monocytes

Lineage tracing and BrdU pulse-chase studies have established a consensus that Ly6C^{hi} monocytes give rise to Ly6C^{low} monocytes (Yona et al., 2012). Yet it remains possible that Ly6C^{low} monocytes arise independent of the Ly6C^{hi} population. The monocyte dendritic cell precursor (MDP) that expresses *Flt3* (CD135), *Cx3cr1* and *Kit* (CD117) gives rise to all mouse monocytes (Hettinger et al., 2013). MDPs undergo further restriction towards the monocyte lineage upon their differentiation into the common monocyte progenitor (cMoP), at which point the expression of FLT3 is lost and Ly6C is gained (Hettinger et al., 2013).

We reasoned that if Ly6C^{low} monocytes arise independently of the Ly6C^{hi} population that we would observe a signature that was common to the Ly6C^{low} monocyte and their progenitor, but not the Ly6C^{hi} monocyte. To test this hypothesis we performed ChIP-Seq on MDP, cMoP, Ly6C^{hi} and Ly6C^{low} monocytes (Figure 1a) using H3K4me2 to define enhancers, and activity with H3K27ac. To assess data quality we visually inspected loci associated with prototypical marker genes for the profiled cell types (Figure 1b). As expected MDPs showed enrichment for H3K27ac at the *Flt3* locus whereas both MDPs and cMoPs showed H3K27ac at the *Kit* locus, both used to sort these populations. In contrast to Ly6C^{low} monocytes, Ly6C^{hi} monocytes and cMoPs show enhancer activity at the *Ly6c2* locus encoding for the Ly6C surface antigen. MDPs also showed activity at the *Ly6c2* locus in spite of low mRNA and cell-surface protein expression (Figure 1a,b), perhaps indicating a priming of this locus prior to transcription. Finally, in Ly6C^{low} monocytes *Cx3cr1* shows marked H3K27ac reflecting the robust Cx3cr1 expression in this population (Carlin et al., 2013).

To gain a global overview of enhancer dynamics during monocyte development H3K4me2 and H3K27ac were quantitated at all 99,462 enhancers defined as H3K4me2 enriched regions greater than 2.5kb from the nearest transcription start site. Differential enrichment (DE) of histone marks was then computed between all pairwise comparisons identifying a total of 620 DE H3K4me2 regions (0.62% of total, Figure S1a) and 9,879 H3K27ac regions (9.93% of total, Figure S1b). Unbiased hierarchical clustering of DE enhancers (Figure 1c, S1c) showed that these changes in H3K27ac are mirrored by more subtle shifts in H3K4me2. *De novo* motif analysis within these defined clusters identified transcriptional processes driving monocyte differentiation (Figure S1d). All enhancer clusters were enriched for ETS (PU.1) motifs. Progenitor-associated enhancers showed restricted over-representation of Myb motifs, which were lost upon Ly6C^{hi} monocyte differentiation, concomitant with the acquisition of CEBP, and KLF motifs. At the global acetylation level

Ly6C^{low} monocytes enhancers were uniquely characterized by over-represented NR4A and Mef2a motifs. Of note we did not observe a signature of enhancer or motif usage that was shared between Ly6C^{low} monocytes and either progenitor but not Ly6C^{hi} monocytes, nor did such a pattern emerge at the transcriptomic level (Figure S2). Instead, the patterns of differential enhancer usage were consistent with a continuous transition between the MDP and Ly6C^{low} monocytes with both the cMoP and Ly6C^{hi} monocytes falling as intermediaries in this cascade. Collectively, these data strongly support the consensus model of monocyte development in which Ly6C^{low} monocytes derive directly from the Ly6C^{hi} monocyte population.

Ly6C^{low} monocytes possess a cell-specific super-enhancer at the *Nr4a1* locus

Super-enhancers (SE) are a recently defined class of highly cell-type specific enhancer (Whyte et al., 2013) that selectively mark genes involved in lineage specification and function. The defining features of SEs include their extended size, adornment with LDTFs and genomic correlates of high gene expression (Hnisz et al., 2013). As Ly6C^{low} monocytes highly express *Nr4a1* and require it for their development (Hanna et al., 2011) we postulated that it is a SE regulated gene. We used H3K27ac to define SEs in Ly6C^{low} monocytes, confirming that *Nr4a1* does overlap a SE (*Nr4a1se;* Figure 2a and S2). Validating the SE characteristics of *Nr4a1se*, we also observed a high density of the MP LDTFs PU.1 and CEBPβ (Figure S3). Enumeration of H3K4me2 and H3K27ac tag counts at *Nr4a1se* in MDP, cMoP, Ly6C^{hi} and Ly6C^{low} monocytes revealed a selective and robust (5-fold) acquisition of H3K27ac in Ly6C^{low} monocytes, demonstrating that *Nr4a1se* is a Ly6C^{low} monocyte-specific SE region (Figure 2b, c).

The formation of SEs represents a confluence of developmental and environmental cues (Hnisz et al., 2015). We leveraged the phenotypic heterogeneity of the diverse MP family to address whether steady-state *Nr4a1* expression may be regulated by distinct mechanisms. First we assessed *Nr4a1* expression in MP populations taken from Lavin *et al* (2014) and our own monocyte subset data. We observed steady-state expression of *Nr4a1* spanning three orders of magnitude (Figure 2d). Importantly *Nr4a1* expression in Ly6C^{hi} monocytes from both datasets (labeled Ly6C^{hi} and Mononocytes) were consistent, facilitating the comparison between datasets. Consistent with previous observations we also observed by far the highest *Nr4a1* expression in Ly6C^{low} monocytes (Hanna et al., 2011).

Next we questioned whether the range of *Nr4a1* mRNA expression was associated with the continuous acquisition of a fixed enhancer signature at *Nr4a1se*, or if Ly6C^{low} monocytes possessed a unique H3K27ac profile. We visualized H3K27ac at *Nr4a1se* in MP populations corresponding to those in Figure 2d (Figure 2e). We observed comparable H3K27ac tag distributions between Ly6C^{hi} monocyte populations, facilitating a qualitative comparison between datasets. Each population was found to differ qualitatively in both the enrichment of histone acetylation and, to varying degrees, also in the histone acetylation ‘fingerprint’ at *Nr4a1se* (Figure 2e). Notably, the most intense H3K27ac signature at *Nr4a1se* was observed in Ly6C^{low} monocytes (Figure 2d,e). Taken together, these findings imply that distinct mechanisms may regulate steady-state *Nr4a1* expression between MP populations.

Nr4a1se domain E2 is a conserved SE sub-domain essential for Ly6C^{low} monocyte development

We sought to identify regions of *Nr4a1se* that regulate *Nr4a1* gene expression in Ly6C^{low} monocytes. Based on PU.1 and C/EBPβ binding in Ly6C^{low} monocytes (Figure S4a) we cloned 12 candidate sequences into luciferase reporters containing a minimal *Nr4a1* promoter (Figure S4b). *Nr4a1se* sub-domains E2, E6, E8 and E9 induced modest but consistent luciferase activity in the myeloid RAW264.7 cell line indicating that these regions may regulate *Nr4a1* in Ly6C^{low} monocytes (Figure 3a). It has been suggested that human CD14^{dim}CD16^{hi} monocytes are homologous to mouse Ly6C^{low} monocytes. This notion is based on global gene expression profiling and observation of the characteristic patrolling behavior in CD14^{dim}CD16^{hi} monocytes (Cros et al., 2010). We reasoned that if CD14^{dim}CD16^{hi} and Ly6C^{low} monocytes are truly orthologous that *Nr4a1* should be regulated by a conserved mechanism. To test this hypothesis we assessed the genetic regulatory state of human DNA sequences orthologous to mouse E2, E6, E8 and E9 in human monocytes using publicly available datasets (Boyle et al., 2008; Schmidl et al., 2014). Human monocyte DNase-Seq clearly shows open chromatin at orthologous regions to mouse E2, E6 and E9 (Figure 3b), however no ortholog for E8 was identified by nucleotide sequence alignment using BLAT. Human E2, E6 and E9 also possessed H3K27ac, and H3K27ac enrichment was greater at E2 and E6 in CD14^{dim}CD16^{hi} monocytes than CD14^{hi}CD16^{neg} monocytes, consistent with the pattern observed between mouse monocyte subsets (Figure 3b). This provides evidence that E2, E6 and E9 are functionally conserved enhancer elements between species, supporting the notion that these regions are important regulators of MP *Nr4a1* gene expression.

To test the *in vivo* functions of E2, E6 and E9 we used the CRISPR-*Cas9* system to generate three mouse strains, each containing a deletion of enhancer sequence to give E2 domain-deficient, E6 domain-deficient and E9 domain-deficient mice respectively (Figure 3c, S4c). Flow cytometry analysis of peripheral monocytes revealed a reduction in monocyte frequencies in E2 domain-deficient, no difference in E9 domain-deficient, and a modest increase in E6 domain-deficient mice (Figure 3d). WT-like monocyte subset ratios were preserved in both E6 domain-deficient and E9 domain-deficient mice, however a striking deficit in Ly6C^{low} monocytes phenocopying the *Nr4a1*$^{-/-}$ strain was present in E2 domain-deficient mice (Figure 3e,f) (Hanna et al., 2011). Therefore the conserved super-enhancer sub-domain E2 is indispensible for Ly6C^{low} monocyte development.

Deletion of enhancer domain E2 decouples inflammation-associated *Nr4a1* gene expression from Ly6C^{low} monocyte-associated *Nr4a1* expression

Current genetic models to study MP *Nr4a1* are based on global *Nr4a1*$^{-/-}$ mice or Cre recombinase mediated deletion of *Nr4a1*$^{flox/flox}$ alleles using myeloid specific Cre transgenes, which include, but are not restricted to *Csf1r, Lyz2* (LysM) and *Cx3cr1*. While these tools ablate MP *Nr4a1* they are non-specific with respect to individual MP subsets (Chow et al., 2011; Yona et al., 2012). Consequently, in models that lack Ly6C^{low} monocytes, *Nr4a1* is also disrupted in macrophages (Figure 4a). As Ly6C^{low} monocytes are absent in E2 domain-deficient mice and *Nr4a1* is a key suppressor of macrophage

inflammatory gene expression we questioned whether E2 domain-deficient macrophages possess wild type-like responses to inflammatory stimuli.

During endotoxic shock macrophage mediated production of inflammatory cytokines ultimately precipitates organ failure and mortality (Jacob et al., 2007). As *Nr4a1*$^{-/-}$ mice are more sensitive to LPS-induced organ failure (Li et al., 2015) we decided to test the role of E2 in this setting. We administered a single high dose of LPS (2.5 mg/kg) to E2 domain-deficient, *Nr4a1*$^{-/-}$, and WT mice by IP injection. All three groups displayed disheveled fur and shivering within the first 72 hours however *Nr4a1*$^{-/-}$ mice showed a significantly higher mortality than both WT and E2 domain-deficient groups, whose symptoms resolved in the 72–120-hour time window (Figure 4b). To understand the role of E2 in the regulation of *Nr4a1* gene expression we measured *Nr4a1* responses to LPS stimulation in thioglycollate-elicited macrophages. WT, E2 domain-heterozygous and E2 domain-deficient macrophages all showed the well-characterized peak of *Nr4a1* mRNA at 1h followed by a return to baseline by 3h (Figure 4c, Pei et al., 2005). Immuno blot analysis also confirmed protein induction in WT and E2 domain-deficient macrophages at 1h following stimulation (Figure 4d). Furthermore, in a dose-response setting (Figure 4e) we observed no differences in *Nr4a1* mRNA expression between WT, E2 domain-heterozygous and E2 domain-deficient macrophages. Finally, following LPS challenge we detected higher expression of *Il12*, *Il1b* and *Nos2* mRNA and iNOS activity in *Nr4a1*$^{-/-}$ mice relative to E2 domain-deficient mice, which were comparable to wild type controls (Figure 4f,g). These studies confirm that the E2 region does not regulate *Nr4a1* expression in response to TLR4 stimulation.

Differential PU.1 binding reveals candidate regulators of Ly6C^{low} monocyte gene expression

We sought to determine the molecular mechanisms regulating *Nr4a1* expression in Ly6C^{low} monocytes. Cooperative interactions between PU.1 and secondary co-factors establish and maintain macrophage enhancer repertoires (Heinz et al., 2010, 2013). Furthermore, differences in SDTF activity elicited within tissue microenvironments are responsible for the diverse range of MP enhancers observed *in vivo* (Gosselin et al., 2014; Lavin et al., 2014). One mechanism for enhancer acquisition involves SDTF driving the formation of latent enhancers associated with *de novo* H3K4me2 and PU.1 binding (Kaikkonen et al., 2013; Ostuni et al., 2013). Thus the subset of *de novo* PU.1 binding events provides valuable information concerning secondary SDTF identity by virtue of motif enrichment (Gosselin et al., 2014).

To define motifs associated with Ly6C^{low} monocytes we determined PU.1 binding profiles in Ly6C^{hi} and Ly6C^{low} monocytes, identifying a total of 65,070 PU.1 peaks. Strict criteria for differential binding led to the identification of 345 Ly6C^{low} monocyte specific PU.1 peaks (Figure 5a) that possess the hallmarks of a latent enhancer repertoire. These include increased H3K4me2 and nucleosome phasing at regions immediately surrounding the PU.1 peaks (Figure S5a); elevated H3K27ac (Figure 5b); and, increased expression of proximal mRNA transcripts (Figure 5c) in Ly6C^{low} monocytes relative to upstream progenitors. Thus, the Ly6C^{low} monocyte PU.1-specific peak profile was associated with enhancers that regulate the Ly6C^{low} monocyte gene expression program. Motifs implicated in Ly6C^{low}

monocyte gene expression were identified using *de novo* motif enrichment analysis on this PU.1 peak set. In strong agreement with our earlier analysis (Figure S1c) we recovered ETS, C/EBP and NR4A motifs (Figure 5d)as expected, alongside IRF, KLF, RUNX and MEF2 motifs. Using our RNA-Seq dataset we identified transcription factors that were expressed in Ly6C^{low} monocytes and could bind to these motifs (Figure 5e), considering the most abundant as our primary candidate. This approach defined *Cebpb*, *Irf5*, *Klf2*, *Mef2a*, *Nr4a1*, *Sfpi1* (PU.1) and *Runx2* as principal regulators of Ly6C^{low} monocyte gene expression.

Klf2 regulates Ly6C^{low} monocyte conversion via E2

To identify transcription factors that regulate *Nr4a1* expression via E2 we overexpressed each candidate with the E2 reporter. *Cebpb, Irf5, Klf2, Mef2a, Nr4a1* and *Runx2* were co-transfected into RAW264.7 macrophages alongside either the *Nr4a1-TSS* or E2-*Nr4a1-TSS* luciferase reporter plasmids. To account for promoter dependent effects of the cDNA and the intrinsic activity of the E2 sequence, an enhancer index was calculated that denotes the difference in the ratio of induced luciferase activity between E2-*Nr4a1-TSS* and *Nr4a1-TSS*. We found that only *Klf2* drove E2-dependent luciferase expression (Figure 6a). Supporting this finding a motif search for the enriched IRF, KLF, RUNX and MEF2 motifs within the E2 region identified a cluster of 3 KLF motifs but failed to find any instances of the other motif classes (Figure S5b).

We chose to investigate the role of KLF factors in Ly6C^{low} monocyte development. KLFs are broadly expressed in Ly6C^{low} monocytes with *Klf2* and *Klf4* being the most abundant (Figure 5e). Owing to the perinatal and embryonic lethality of *Klf2*$^{-/-}$ and *Klf4*$^{-/-}$ mice we assessed monocyte frequencies in myeloid-specific *Lyz2-cre Klf2*$^{flox/flox}$ and *Lyz2-cre Klf4*$^{flox/flox}$ mice (Liao et al., 2011; Mahabeleshwar et al., 2011). Flow cytometric analysis of *Lyz2-cre Klf4*$^{flox/flox}$ blood monocytes showed a decrease in both populations (Figure 6b), consistent with previous reports (Alder et al., 2008). In *Lyz2-cre Klf2*$^{flox/flox}$ mice Ly6C^{hi} monocytes were unaffected however Ly6C^{low} monocytes were partially reduced (Figure 6b). Similar results were also observed in the bone marrow of *Lyz2-cre Klf2*$^{flox/flox}$ and *Lyz2-cre Klf4*$^{flox/flox}$ mice and in bone marrow chimeric mice retrovirally transduced with shRNA targeting *Klf2* and *Klf4* (Figure S6a,b).

We have previously observed incomplete deletion of loxP-flanked genes in blood monocytes using the *Lyz2-cre* system (Hanna et al., 2015). Therefore the differences in monocyte frequencies between *Lyz2-cre Klf2*$^{flox/flox}$ and *Lyz2-cre Klf4*$^{flox/flox}$ mice may either reflect intrinsic differences in the ability of each gene to regulate monocyte development, or simply the abundance of each TF in each subset. To address this we measured *Klf2* and *Klf4* mRNA in Ly6C^{hi} and Ly6C^{low} monocytes sorted from *Lyz2-cre Klf2*$^{flox/flox}$ and *Lyz2-cre Klf4*$^{flox/flox}$ mice using primers that span the loxP-flanked exon to determine recombination efficiency. In *Lyz2-cre Klf2*$^{flox/flox}$ mice 72% and 91% loss of *Klf2* mRNA was observed for Ly6C^{hi} and Ly6C^{low} monocytes respectively (Figure S6c). Thus the selective loss of Ly6C^{low} monocytes in *Lyz2-cre Klf2*$^{flox/flox}$ mice is not consistent with the incomplete deletion of *Klf2* in Ly6C^{hi} monocytes. A role for *Klf2* in Ly6C^{hi} to Ly6C^{low} monocyte conversion is also consistent with the induction of *Klf2* gene expression in the transition between subsets (Figure 5e). In *Lyz2-cre Klf4*$^{flox/flox}$ mice *Klf4* mRNA was reduced by 63%

and 69% in Ly6C^{hi} and Ly6C^{low} monocytes respectively (Figure S6d). Although *Lyz2-cre Klf4$^{flox/flox}$* mice possessed fewer Ly6C^{low} monocytes it is not clear whether this resulted from fewer precursor Ly6C^{hi} monocytes, a decrease in Ly6C^{hi} to Ly6C^{low} monocyte conversion, or both. We reasoned that if *Klf2* or *Klf4* regulated Ly6C^{hi} to Ly6C^{low} monocyte conversion via *Nr4a1* that *Klf2* or *Klf4* gene expression would predict *Nr4a1* expression. Indeed, *Nr4a1* mRNA expression was lower in Ly6C^{hi} monocytes derived from *Lyz2-cre Klf2$^{flox/flox}$* mice, but not *Lyz2-cre Klf4$^{flox/flox}$* mice (Figure 6c). Subsequent investigation revealed a significant positive correlation between *Klf2* and *Nr4a1* transcript expression in both monocyte subsets, however no such relationship was found between *Klf4* and *Nr4a1* gene expression (Figure 6d,e and S6e,f).

While of a preliminary nature, these correlative findings suggest that *Klf2* regulates Ly6C^{low} monocyte development via E2. Given our evidence for a conserved mechanism of *Nr4a1* gene expression between species (Figure 3b) we predict that *KLF2* expression follows a similar pattern in human monocyte subsets.

Interrogation of microarray data for *KLF2* in human monocytes confirmed this hypothesis, showing significantly higher *KLF2* expression in human CD14^{dim}CD16^{hi} monocytes (Figure 6f).

E2 is a monocyte-specific enhancer

E2 regulates *Nr4a1* expression in Ly6C^{low} monocytes but not in response to LPS stimulation. Furthermore, at steady state, macrophage *Nr4a1* expression spanned three orders of magnitude. To determine the extent to which E2 was Ly6C^{low} monocyte specific we measured *Nr4a1* expression in various MP populations from E2 domain-deficient mice. Blood monocytes, F4/80^{hi} large, F4/80^{int} small peritoneal macrophages (LPM and SPM respectively), CD11c^{+} lung alveolar macrophages, and F4/80^{+} splenic red pulp macrophages were selected (Figure 7a). In line with previous observations (Tacke et al., 2015) macrophage frequencies were largely unchanged in *Nr4a1$^{-/-}$* mice, except for moderately fewer F4/80^{hi} LPM (Figure S7a). RT-PCR analysis captured the expected range of *Nr4a1* expression between macrophage populations (Figure 7b). Strikingly however no difference in *Nr4a1* mRNA was detected between tissue macrophages, except for moderately lower expression in E2 domain-deficient splenic macrophages. In contrast to this a substantial reduction in steady state *Nr4a1* mRNA expression was observed in both Ly6C^{hi} and Ly6C^{low} monocytes (Figure 7c) showing that E2 is a monocyte-specific enhancer.

We recently reported that Ly6C^{low} monocytes prevented cancer metastasis to the lung (Hanna et al., 2015). To demonstrate the utility of the E2 domain-deficient model to study Ly6C^{low} monocytes we assessed tumor burden in mice using a well-established model of metastasis. B16F10 melanoma cells were intravenously injected into WT, *Nr4a1$^{-/-}$* and E2 domain-deficient mice. 18 days after challenge mice were sacrificed and tumor burden was measured by histology. Both *Nr4a1$^{-/-}$* and E2 domain-deficient mice showed a loss of Ly6C^{low} monocytes (Figure S7b) and significantly higher tumor burden than WT (Figure 7d,e) however no difference was observed between *Nr4a1$^{-/-}$* and E2 domain-deficient mice. Consistent with a critical role for Ly6C^{low} monocytes in controlling metastasis, the differences are explained by fewer tumor regions rather than tumor size (Figure S7c,d).

Therefore the E2 domain-deficient model effectively decouples *Nr4a1*-dependent inflammatory phenotypes from Ly6C^{low} monocyte function, providing an improved tool to study the function of these cells. In contrast to conditional deletion strategies using the Cre-Lox system, enhancer targeting confers an unprecedented degree of specificity, enabling the causal inference of individual MP subsets in disease.

Discussion

During our investigation into the transcriptional regulatory pathways of Ly6C^{low} monocyte development we identified E2 as a single domain that is absolutely required for Ly6C^{low} monocyte development. We also observed distinct, cell-subset specific, patterns of H3K27ac at the *Nr4a1se* locus leading us to investigate whether *Nr4a1* gene expression is controlled by distinct mechanisms between MP subsets. E2 domain-deficient mice lack Ly6C^{low} monocytes, yet macrophage *Nr4a1* expression was largely unaffected during steady state and during inflammation. This implies a modular structure for the *Nr4a1* locus control region *Nr4a1se* and is consistent with a recent analysis of several SEs showing that these regions consist of multiple sub-domains (Hnisz et al., 2015). Disrupting these sub-domains differentially affected target gene expression depending upon the locus. For example at *Sik1*, additive effects between sub-domains contribute towards the stable induction of gene expression, whereas at *Prdm14*, mRNA expression was regulated almost entirely by one of five sub-domains (Hnisz et al., 2015). Our study has identified three active and conserved MP enhancers upstream of *Nr4a1*; E2, E6 and E9, yet only E2 regulates Ly6C^{low} monocyte development. This highlights the importance of detailed molecular analyses to establish the relevance of individual enhancer elements, and TF binding motifs within these elements. Whether E6 and E9 regulate MP *Nr4a1* gene expression in response to other stimuli is a line of future enquiry.

Our studies suggest that KLF transcription factors regulate *Nr4a1* gene expression via E2. Ly6C^{low} monocyte enhancers were enriched for KLF motifs, and these motifs were present in E2. Multiple KLF family members are expressed in Ly6C^{low} monocytes, which may act redundantly at E2. In Ly6C^{low} monocytes *Klf2* and K*lf4* were the most abundant family members, thus we investigated the roles of these genes. Both *Klf2* and *Klf4* regulate macrophage inflammatory gene expression by inhibiting p300 and PCAF recruitment to NF-kB (Das et al., 2006; Liao et al., 2011). The different roles ascribed to each factor may arise from the different contexts in which they are expressed. *Klf4* was induced during Ly6C^{hi} monocyte differentiation, and was further up-regulated in macrophages by IL-4. In this context *Klf4* regulates Ly6C^{hi} monocyte development and facilitates the M2 program of macrophage activation (Feinberg et al., 2007; Liao et al., 2011). *Klf2* however is expressed in circulating monocytes, and strongly reduced by hypoxia leading to increased NF-kB and Hif-1 activity (Mahabeleshwar et al., 2011).

Our findings suggest non-redundant roles for *Klf2* and *Klf4* in in monocyte development. *Klf4* expression is high in both monocyte subsets and *Lyz2-cre Klf4$^{flox/flox}$* mice have fewer monocytes. However, the ratio of Ly6C^{hi} to Ly6C^{low} monocytes, and Ly6C^{low} monocyte *Nr4a1* expression were not affected in *Lyz2-cre Klf4$^{flox/flox}$* mice However, depletion of *Klf2* facilitated a selective loss of Ly6C^{low} monocytes and *Klf2* mRNA expression was

predictive of *Nr4a1* expression, implying a causal relationship between *Klf2* and *Nr4a1*. Despite repeated attempts we were not able to obtain successful immunoprecipitation of KLF2 at the *Nr4a1se* locus due to an absence of high-quality commercial antibodies; neither was overexpression of *Klf2* sufficient to up-regulate *Nr4a1* mRNA *in vitro* (data not shown). These preliminary findings suggest that *Klf2* acts via E2 locus and is necessary, but not sufficient, for Ly6C^{low} monocyte development. The identification of additional critical co-factors acting via E2, the *Nr4a1* promoter or elsewhere will pave the way for a more detailed mechanistic understanding of how E2 regulates *Nr4a1* gene expression in Ly6C^{low} monocyte development.

MP occupy all tissues of the body where these cells perform specialized functions to facilitate homeostasis. For example, Ly6C^{low} monocytes maintain vascular integrity by facilitating removal of damaged endothelium (Carlin et al., 2013), alveolar macrophages maintain lung function by clearing surfactants (Nakamura et al., 2013), red pulp macrophages contribute to iron homeostasis by recycling erythrocytes (Kohyama et al., 2009), whereas the microglia's dedicated functions include supporting brain function by synaptic pruning (Paolicelli et al., 2011). These specialized functions are imparted by tissue-specific LTDFs; Ly6C^{low} monocytes require *Nr4a1* (Hanna et al., 2011); alveolar macrophages rely upon PPARγ (Schneider et al., 2014); splenic red pulp-macrophages macrophages need *Spic* (Kohyama et al., 2009); while resident peritoneal macrophages depend upon the transcription factor GATA6 (Okabe and Medzhitov, 2014).

In some cases, such as *for Gata6* and *Spic*, LDTF expression within the MP system is cell-specific such that macrophage-specific deletion of the factor is sufficient to study the function of the associated subset. However, for the most part both the expression and requirement of key MP TFs are not cell-specific. Epigenetic analyses of MP subsets reveals shared motif usage and co-expression of cognate TFs over multiple subsets (Lavin et al., 2014). For example PPAR motifs are enriched in alveolar and renal macrophage enhancers and PPARγ regulates both alveolar macrophage and osteoclast differentiation (Schneider et al., 2014; Wan et al., 2007). Disease processes complicate matters further by invoking dynamic transcription factor expression and altering requirements, in this context PPARγ is up-regulated by IL-4 and controls alternative macrophage activation (Odegaard et al., 2007). Similarly, *Nr4a1* is required for Ly6C^{low} monocyte development and is also induced by LPS (Hanna et al., 2011; Pei et al., 2005). These pleiotropic effects limit our ability to study individual MP subsets and the lack of specificity provided by current myeloid Cre transgenes presents a problem when attempting to target individual subsets.

We have shown that enhancer targeting can overcome these limitations. Our approach leverages the unique enhancer repertoires resulting from the exclusive environment each MP subset occupies. We have shown that targeting cell-specific SE sub-domains within key LDTFs functionally decouples cell-specific aspects of gene expression while retaining physiological characteristics of gene function relevant to neighbouring cell subsets. In our case, targeting the E2 sub-domain provides a loss-of-function tool to study Ly6C^{low} monocytes that preserves both *Nr4a1* expression in other MP populations and the rapid kinetics of *Nr4a1* expression in response to LPS signaling. Conceptually this strategy can be

applied to any scenario in which gene expression is regulated by distinct enhancer sequences as an approach to study gene function amongst closely related cell types.

Experimental procedures

Mice

C57BL/6J mice were purchased from the Jackson laboratory. Congenic *Nr4a1*$^{-/-}$ mice previously described (Hanna *et al.*, 2011) and enhancer deficient mice were maintained in-house. All experiments followed guidelines of the La Jolla Institute for Allergy and Immunology (LIAI) Animal Care and Use Committee, and approval for use of rodents was obtained from LIAI according to criteria outlined in the Guide for the Care and Use of Laboratory Animals from the National Institutes of Health. Mice were euthanized by CO2 inhalation.

Cell sorting

Mice were sacrificed by CO_2 inhalation and bone marrow or blood extracted into DPBS + 2mM ETDA. Following RBC lysis cells were blocked and stained for surface antigens and purified by flow cytometry as described in the figures as described in the extended experimental procedures.

Thioglycollate elicited macrophages

Thioglycollate elicited macrophages were elicited by intraperitoneal injection of 1ml 4% Brewer's Thioglycollate Medium. 5 days after injection macrophages were harvested and cultured as described in the extended experimental procedures.

RNA isolation and RNA-Seq

Sorted cells were immediately spun down and stored in Trizol. RNA was extracted using DirectZol columns (Zymo Research). RNA was prepared for sequencing using the TruSeq v2 kit (Illumina).

ChIP-Seq

Histone ChIP was performed using the protocol described in (Gilfillan et al., 2012) and transcription factor ChIP performed essentially as described in (Gosselin et al., 2014), with modifications described in the extended methods. ChIP-Seq libraries were prepared using the ThruPlex-FD kit (Rubicon Genomics).

Molecular cloning and overexpression studies

Enhancers were amplified by PCR and cloned into the SalI and Bamh1 sites of a pGL4.10 series vector described in (Heinz *et al.*, 2013) modified to contain an *Nr4a1* minimal promoter (300 bp) and 5′UTR, please see table S1. Transfection assays were performed in murine RAW264.7 macrophages using Lipofectamine LTX. cDNA expression vectors were obtained from Origene. Full details are in the extended experimental procedures.

CRISPR mouse generation

Mouse genome editing was performed essentially as described with minor modifications (Concepcion et al., 2015; Wang et al., 2013). Four sgRNA (two pairs targeting each enhancer flanking region) were injected into embryos of supervoulated C57BL/6 mice along with *Cas9* mRNA (Life Technologies) at the UCSD transgenic core facility. Please refer to table S2. Founder mice containing the desired deletions identified by PCR (table S3) were mated with C57BL/6 and offspring thereafter maintained via sibling mating.

Bone marrow chimeras

Bone marrow was shipped on ice as described in the extended experimental methods. Recipient mice were lethally irradiated and bone marrow transplanted by retroorbital injection. Mice were allowed to recover for at least 6 weeks before performing experiments.

Cancer study

300,000 B16F10 melanoma cells were injected via tail vein into recipient mice. Lungs were harvested in zinc buffered formalin and mounted into paraffin blocks. Sections were stained with H&E and slides were scanned with an AxioScan Z1 (Zeiss), see extended experimental procedures.

Endotoxin sensitivity assay

Ultrapure LPS-EB (Invivogen) was made up in PBS and injected IP. Mice were monitored three times daily for the first 72 hours and twice daily thereafter.

Bioinformatics data analysis

FASTQ files were mapped to the mouse mm10 reference genome using RNA-STAR for RNA-Seq experiments, or Bowtie for ChIP-Seq studies. RNA-Seq expression was quantitated using featureCounts and differential expression analyzed using edgeR. ChIP-Seq analysis was performed using HOMER. For full details see extended experimental procedures.

Supplementary Material

Refer to Web version on PubMed Central for supplementary material.

Acknowledgments

We would like to acknowledge the flow cytometry core and sequencing core facilities as well as the UCSD transgenic core facility. Funding sources: R01HLx118765, R01CA202987 and R01HL112039 to CCH; R01DK091183, R01CA17390 and R01HL088093 to CKG; R00HL123485 to CER; R01GM086912 to BAH; R01HL086548 and R01075427 to MKJ. AHA Fellowships 16POST27630002 to GDT and 12DG12070005 to RNH. KDR was supported in part by a Ruth L. Kirschstein National Research Service Award (NRSA) Institutional Predoctoral Training Grant, T32 GM008666, from the National Institute of General Medical Sciences.

References

Alder JK, Georgantas RW, Hildreth RL, Kaplan IM, Morisot S, Yu X, McDevitt M, Civin CI. Kruppel-Like Factor 4 Is Essential for Inflammatory Monocyte Differentiation In Vivo. J Immunol. 2008; 180:5645–5652. [PubMed: 18390749]

Amit I, Winter DR, Jung S. The role of the local environment and epigenetics in shaping macrophage identity and their effect on tissue homeostasis. Nat Immunol. 2016; 17:18–25. [PubMed: 26681458]

Andersson R, Gebhard C, Miguel-Escalada I, Hoof I, Bornholdt J, Boyd M, Chen Y, Zhao X, Schmidl C, Suzuki T, et al. An atlas of active enhancers across human cell types and tissues. Nature. 2014; 507:455–461. [PubMed: 24670763]

Boyle AP, Davis S, Shulha HP, Meltzer P, Margulies EH, Weng Z, Furey TS, Crawford GE. High-resolution mapping and characterization of open chromatin across the genome. Cell. 2008; 132:311–322. [PubMed: 18243105]

Carlin LM, Stamatiades EG, Auffray C, Hanna RN, Glover L, Vizcay-Barrena G, Hedrick CC, Cook HT, Diebold S, Geissmann F. Nr4a1-Dependent Ly6Clow Monocytes Monitor Endothelial Cells and Orchestrate Their Disposal. Cell. 2013; 153:362–375. [PubMed: 23582326]

Chow A, Brown BD, Merad M. Studying the mononuclear phagocyte system in the molecular age. Nat Rev Immunol. 2011; 11:788–798. [PubMed: 22025056]

Concepcion D, Ross KD, Hutt KR, Yeo GW, Hamilton BA. Nxf1 natural variant E610G is a semi-dominant suppressor of IAP-induced RNA processing defects. PLoS Genet. 2015; 11:e1005123. [PubMed: 25835743]

Creyghton MP, Cheng AW, Welstead GG, Kooistra T, Carey BW, Steine EJ, Hanna J, Lodato MA, Frampton GM, Sharp PA, et al. Histone H3K27ac separates active from poised enhancers and predicts developmental state. Proc Natl Acad Sci. 2010

Cros J, Cagnard N, Woollard K, Patey N, Zhang SY, Senechal B, Puel A, Biswas SK, Moshous D, Picard C, et al. Human CD14dim monocytes patrol and sense nucleic acids and viruses via TLR7 and TLR8 receptors. Immunity. 2010; 33:375–386. [PubMed: 20832340]

Das H, Kumar A, Lin Z, Patino WD, Hwang PM, Feinberg MW, Majumder PK, Jain MK. Kruppel-like factor 2 (KLF2) regulates proinflammatory activation of monocytes. Proc Natl Acad Sci U S A. 2006; 103:6653–6658. [PubMed: 16617118]

Feinberg MW, Wara AK, Cao Z, Lebedeva MA, Rosenbauer F, Iwasaki H, Hirai H, Katz JP, Haspel RL, Gray S, et al. The Kruppel-like factor KLF4 is a critical regulator of monocyte differentiation. EMBO J. 2007; 26:4138–4148. [PubMed: 17762869]

Geissmann F, Manz MG, Jung S, Sieweke MH, Merad M, Ley K. Development of monocytes, macrophages, and dendritic cells. Science. 2010; 327:656–661. [PubMed: 20133564]

Gilfillan GD, Hughes T, Sheng Y, Hjorthaug HS, Straub T, Gervin K, Harris JR, Undlien DE, Lyle R. Limitations and possibilities of low cell number ChIP-seq. BMC Genomics. 2012; 13:645. [PubMed: 23171294]

Gosselin D, Link VM, Romanoski CE, Fonseca GJ, Eichenfield DZ, Spann NJ, Stender JD, Chun HB, Garner H, Geissmann F, et al. Environment Drives Selection and Function of Enhancers Controlling Tissue-Specific Macrophage Identities. Cell. 2014; 159:1327–1340. [PubMed: 25480297]

Hanna RN, Carlin LM, Hubbeling HG, Nackiewicz D, Green AM, Punt JA, Geissmann F, Hedrick CC. The transcription factor NR4A1 (Nur77) controls bone marrow differentiation and the survival of Ly6C- monocytes. Nat Immunol. 2011; 12:778–785. [PubMed: 21725321]

Hanna RN, Shaked I, Hubbeling HG, Punt JA, Wu R, Herrley E, Zaugg C, Pei H, Geissmann F, Ley K, et al. NR4A1 (Nur77) deletion polarizes macrophages toward an inflammatory phenotype and increases atherosclerosis. Circ Res. 2012; 110:416–427. [PubMed: 22194622]

Hanna RN, Cekic C, Sag D, Tacke R, Thomas GD, Nowyhed H, Herrley E, Rasquinha N, McArdle S, Wu R, et al. Patrolling monocytes control tumor metastasis to the lung. Science. 2015

Heintzman ND, Stuart RK, Hon G, Fu Y, Ching CW, Hawkins RD, Barrera LO, Van Calcar S, Qu C, Ching KA, et al. Distinct and predictive chromatin signatures of transcriptional promoters and enhancers in the human genome. Nat Genet. 2007; 39:311–318. [PubMed: 17277777]

Heinz S, Benner C, Spann N, Bertolino E, Lin YC, Laslo P, Cheng JX, Murre C, Singh H, Glass CK. Simple combinations of lineage-determining transcription factors prime cis-regulatory elements required for macrophage and B cell identities. Mol Cell. 2010; 38:576–589. [PubMed: 20513432]

Heinz S, Romanoski CE, Benner C, Allison KA, Kaikkonen MU, Orozco LD, Glass CK. Effect of natural genetic variation on enhancer selection and function. Nature. 2013

Hettinger J, Richards DM, Hansson J, Barra MM, Joschko AC, Krijgsveld J, Feuerer M. Origin of monocytes and macrophages in a committed progenitor. Nat Immunol. 2013; 14:821–830. [PubMed: 23812096]

Hnisz D, Abraham BJ, Lee TI, Lau A, Saint-André V, Sigova AA, Hoke HA, Young RA. Super-enhancers in the control of cell identity and disease. Cell. 2013; 155:934–947. [PubMed: 24119843]

Hnisz D, Schuijers J, Lin CY, Weintraub AS, Abraham BJ, Lee TI, Bradner JE, Young RA. Convergence of Developmental and Oncogenic Signaling Pathways at Transcriptional Super-Enhancers. Mol Cell. 2015; 58:362–370. [PubMed: 25801169]

Jacob A, Zhou M, Wu R, Halpern VJ, Ravikumar TS, Wang P. PRO-INFLAMMATORY CYTOKINES FROM KUPFFER CELLS DOWNREGULATE HEPATOCYTE EXPRESSION OF ADRENOMEDULLIN BINDING PROTEIN-1. Biochim Biophys Acta. 2007; 1772:766–772. [PubMed: 17490866]

Kaikkonen MU, Spann NJ, Heinz S, Romanoski CE, Allison KA, Stender JD, Chun HB, Tough DF, Prinjha RK, Benner C, et al. Remodeling of the Enhancer Landscape during Macrophage Activation Is Coupled to Enhancer Transcription. Mol Cell. 2013; 51:310–325. [PubMed: 23932714]

Kohyama M, Ise W, Edelson BT, Wilker PR, Hildner K, Mejia C, Frazier WA, Murphy TL, Murphy KM. Role for Spi-C in the development of red pulp macrophages and splenic iron homeostasis. Nature. 2009; 457:318–321. [PubMed: 19037245]

Lavin Y, Winter D, Blecher-Gonen R, David E, Keren-Shaul H, Merad M, Jung S, Amit I. Tissue-Resident Macrophage Enhancer Landscapes Are Shaped by the Local Microenvironment. Cell. 2014; 159:1312–1326. [PubMed: 25480296]

Li L, Liu Y, Chen H, Li F, Wu J, Zhang H, He J, Xing Y, Chen Y, Wang W, et al. Impeding the interaction between Nur77 and p38 reduces LPS-induced inflammation. Nat Chem Biol. 2015; 11:339–346. [PubMed: 25822914]

Liao X, Sharma N, Kapadia F, Zhou G, Lu Y, Hong H, Paruchuri K, Mahabeleshwar GH, Dalmas E, Venteclef N, et al. Krüppel-like factor 4 regulates macrophage polarization. J Clin Invest. 2011; 121:2736–2749. [PubMed: 21670502]

Mahabeleshwar GH, Kawanami D, Sharma N, Takami Y, Zhou G, Shi H, Nayak L, Jeyaraj D, Grealy R, White M, et al. The myeloid transcription factor KLF2 regulates the host response to polymicrobial infection and endotoxic shock. Immunity. 2011; 34:715–728. [PubMed: 21565532]

Muller PA, Koscsó B, Rajani GM, Stevanovic K, Berres ML, Hashimoto D, Mortha A, Leboeuf M, Li XM, Mucida D, et al. Crosstalk between muscularis macrophages and enteric neurons regulates gastrointestinal motility. Cell. 2014; 158:300–313. [PubMed: 25036630]

Nakamura A, Ebina-Shibuya R, Itoh-Nakadai A, Muto A, Shima H, Saigusa D, Aoki J, Ebina M, Nukiwa T, Igarashi K. Transcription repressor Bach2 is required for pulmonary surfactant homeostasis and alveolar macrophage function. J Exp Med. 2013; 210:2191–2204. [PubMed: 24127487]

Odegaard JI, Chawla A. Alternative macrophage activation and metabolism. Annu Rev Pathol. 2011; 6:275–297. [PubMed: 21034223]

Odegaard JI, Ricardo-Gonzalez RR, Goforth MH, Morel CR, Subramanian V, Mukundan L, Red Eagle A, Vats D, Brombacher F, Ferrante AW, et al. Macrophage-specific PPARgamma controls alternative activation and improves insulin resistance. Nature. 2007; 447:1116–1120. [PubMed: 17515919]

Okabe Y, Medzhitov R. Tissue-Specific Signals Control Reversible Program of Localization and Functional Polarization of Macrophages. Cell. 2014; 157:832–844. [PubMed: 24792964]

Okabe Y, Medzhitov R. Tissue biology perspective on macrophages. Nat Immunol. 2016; 17:9–17. [PubMed: 26681457]

Ostuni R, Piccolo V, Barozzi I, Polletti S, Termanini A, Bonifacio S, Curina A, Prosperini E, Ghisletti S, Natoli G. Latent Enhancers Activated by Stimulation in Differentiated Cells. Cell. 2013; 152:157–171. [PubMed: 23332752]

Paolicelli RC, Bolasco G, Pagani F, Maggi L, Scianni M, Panzanelli P, Giustetto M, Ferreira TA, Guiducci E, Dumas L, et al. Synaptic pruning by microglia is necessary for normal brain development. Science. 2011; 333:1456–1458. [PubMed: 21778362]

Parkhurst CN, Yang G, Ninan I, Savas JN, Yates JR III, Lafaille JJ, Hempstead BL, Littman DR, Gan WB. Microglia Promote Learning-Dependent Synapse Formation through Brain-Derived Neurotrophic Factor. Cell. 2013; 155:1596–1609. [PubMed: 24360280]

Pei L, Castrillo A, Chen M, Hoffmann A, Tontonoz P. Induction of NR4A orphan nuclear receptor expression in macrophages in response to inflammatory stimuli. J Biol Chem. 2005; 280:29256–29262. [PubMed: 15964844]

Perdiguero EG, Geissmann F. The development and maintenance of resident macrophages. Nat Immunol. 2016; 17:2–8. [PubMed: 26681456]

Schmidl C, Renner K, Peter K, Eder R, Lassmann T, Balwierz PJ, Itoh M, Nagao-Sato S, Kawaji H, Carninci P, et al. Transcription and enhancer profiling in human monocyte subsets. Blood blood. 2014 2013–02 – 484188.

Schneider C, Nobs SP, Kurrer M, Rehrauer H, Thiele C, Kopf M. Induction of the nuclear receptor PPAR-γ by the cytokine GM-CSF is critical for the differentiation of fetal monocytes into alveolar macrophages. Nat Immunol. 2014; 15:1026–1037. [PubMed: 25263125]

Sica A, Mantovani A. Macrophage plasticity and polarization: in vivo veritas. J Clin Invest. 2012; 122:787–795. [PubMed: 22378047]

Tacke R, Hilgendorf I, Garner H, Waterborg C, Park K, Nowyhed H, Hanna RN, Wu R, Swirski FK, Geissmann F, et al. The transcription factor NR4A1 is essential for the development of a novel macrophage subset in the thymus. Sci Rep. 2015; 5:10055. [PubMed: 26091486]

Wan Y, Chong LW, Evans RM. PPAR-gamma regulates osteoclastogenesis in mice. Nat Med. 2007; 13:1496–1503. [PubMed: 18059282]

Wang H, Yang H, Shivalila CS, Dawlaty MM, Cheng AW, Zhang F, Jaenisch R. One-step generation of mice carrying mutations in multiple genes by CRISPR/Cas-mediated genome engineering. Cell. 2013; 153:910–918. [PubMed: 23643243]

Whyte WA, Orlando DA, Hnisz D, Abraham BJ, Lin CY, Kagey MH, Rahl PB, Lee TI, Young RA. Master transcription factors and mediator establish super-enhancers at key cell identity genes. Cell. 2013; 153:307–319. [PubMed: 23582322]

Yona S, Kim KW, Wolf Y, Mildner A, Varol D, Breker M, Strauss-Ayali D, Viukov S, Guilliams M, Misharin A, et al. Fate Mapping Reveals Origins and Dynamics of Monocytes and Tissue Macrophages under Homeostasis. Immunity. 2012

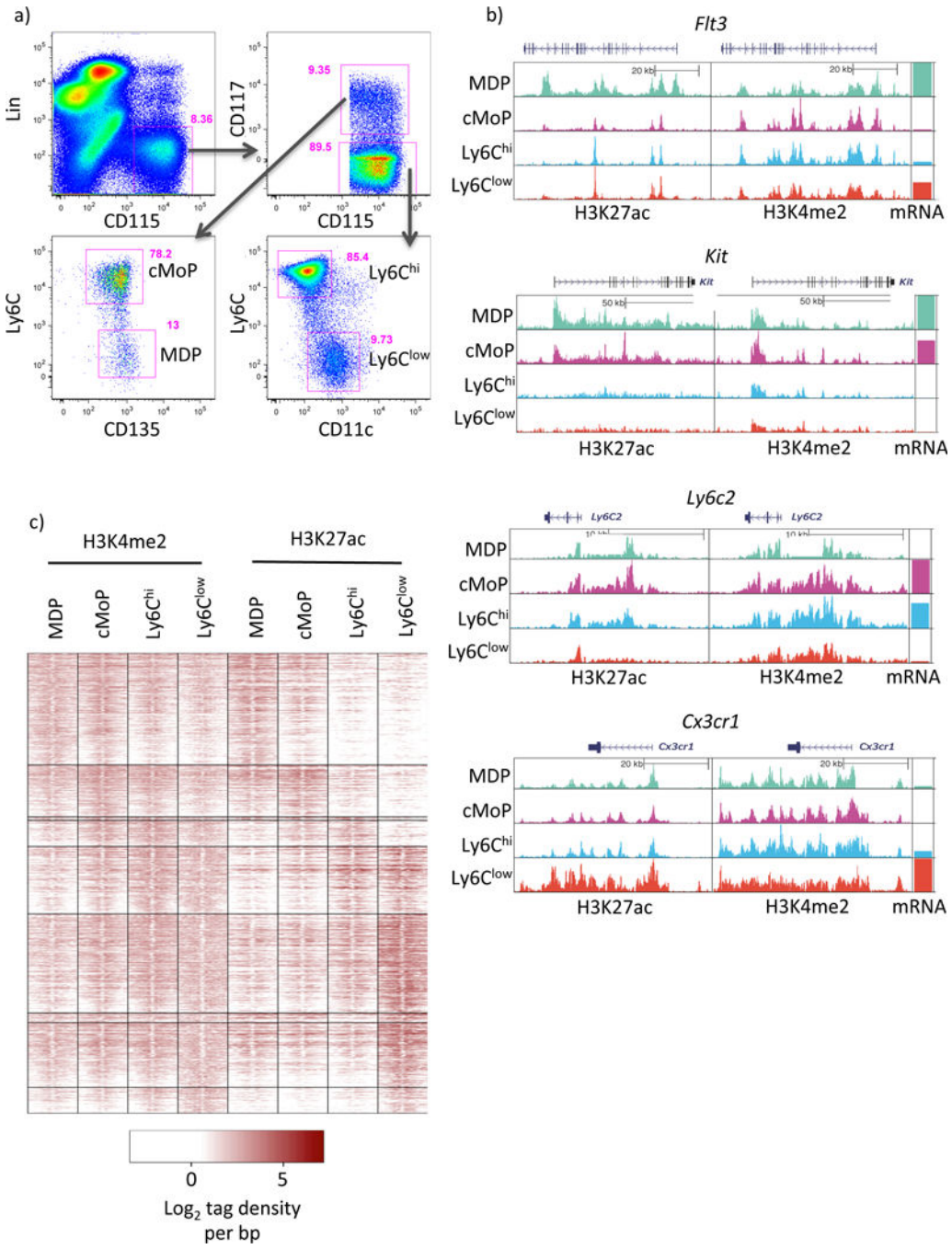

Figure 1. Epigenomic profiling of Mo subsets and progenitors supports the model of Ly6C^{hi} to Ly6C^{low} Mo conversion

a) Gating strategy used to sort monocytes and upstream progenitors. Cells were previously gated on live singlets (using a FSC-W versus FSC-A gate). b) UCSC genome browser screenshots showing H3K27ac and H3K4me2 tag distributions at key lineage genes. c) Distribution of H3K4me2 and H3K27ac tags ±1kb from PU.1 peak centers in DE enhancers. Please see supplementary figures S1 and S2.

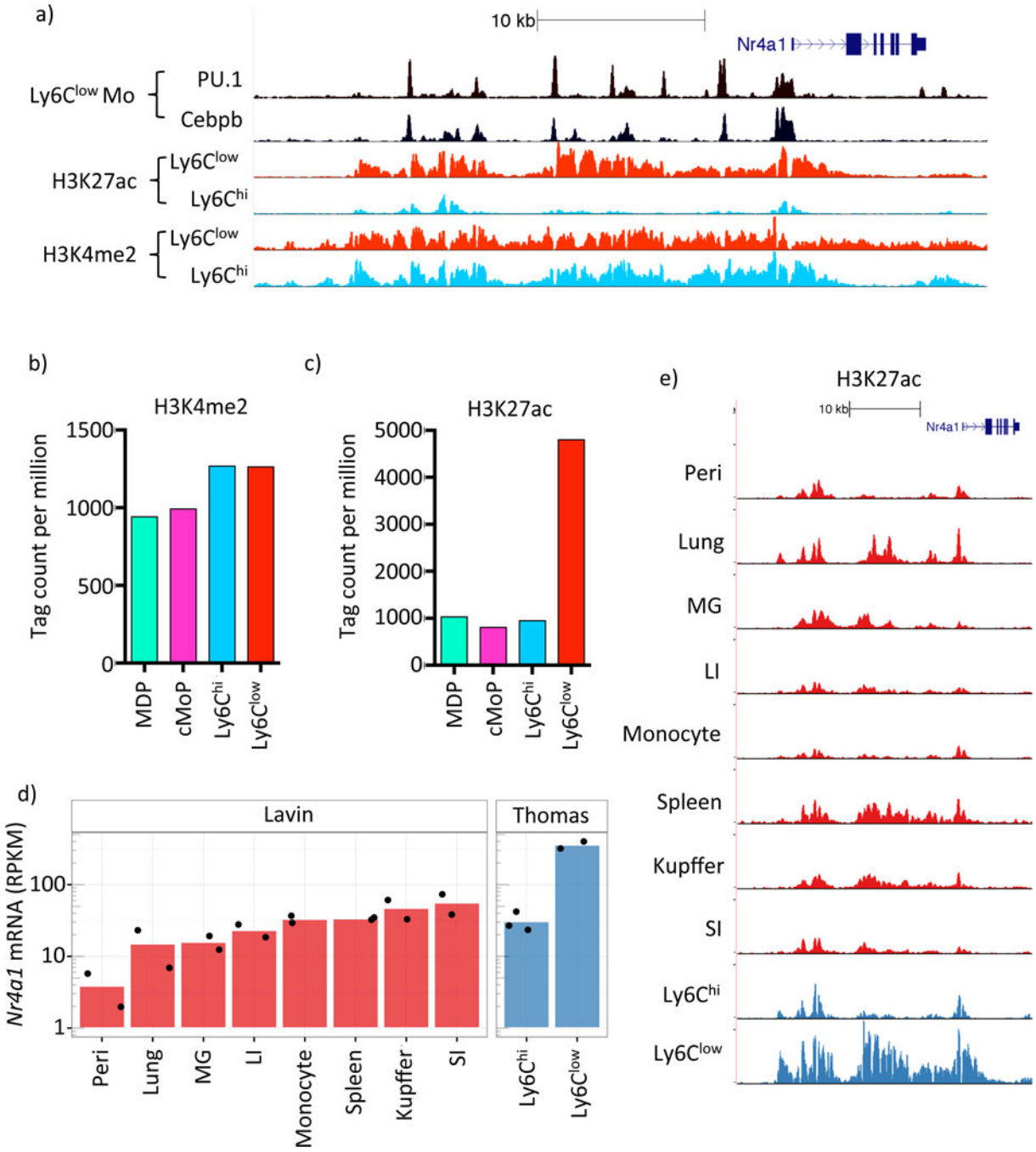

Figure 2. Ly6C^{low} Mo possess a cell-specific SE at the *Nr4a1* locus

a) UCSC genome browser screenshot of the *Nr4a1* locus depicting Ly6C^{low} Mo PU.1 and C/EBPβ binding and H3K4me2 and H3K27ac in both Ly6C^{hi} and Ly6C^{low} Mo. b) and c) H3K4me2 and H3K27ac tag counts at *Nr4a1se* in MDP, cMoP, Ly6C^{hi} and Ly6C^{low} Mo. d) mRNA-Seq expression of *Nr4a1* in various tissue macrophage subsets taken from Lavin *et al* (2014), labeled 'Lavin', and from our data, labeled 'Thomas' (Peri= peritoneal macrophage, MG= microglia, LI= large intestine, SI= small intestine). e) H3K27ac at *Nr4a1se* for the same MP populations as in d). Please refer to supplementary figure S3.

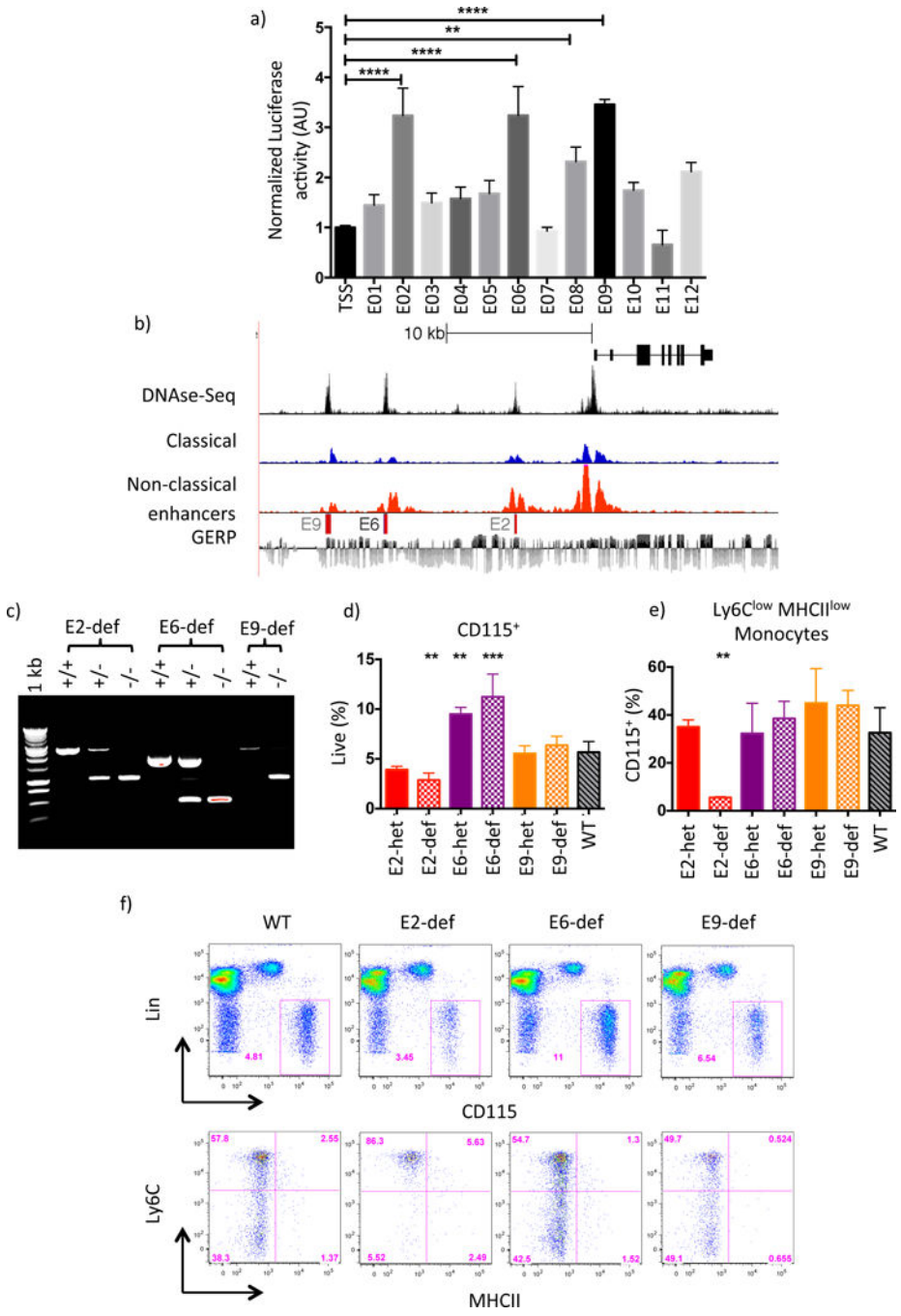

Figure 3. Identification of a conserved SE sub-domain essential for Ly6C^{low} Mo development

a) Relative luciferase activity in RAW264.7 cells of candidate enhancer regions cloned into pGL4.*Nr4a1* vector. Results shown are averaged over 2 independent experiments. Error bars represent SD, P-values calculated by 2-way anova * P<0.05, **P<0.01, ****P<0.0001. b) UCSC genome browser screenshot of the human *Nr4a1* locus. H3K27ac tracks for CD14^{+}CD16^{dim} (classical) and CD14^{dim}CD16^{+} (non-classical) Mo are shown alongside BLAT alignments of nucleosome-free DNA sequence obtained from mouse E2, E6 and E9. Mo DNase-Seq data were taken from (Boyle *et al*, 2008); nucleotide sequence conservation

is indicated using the GERP track. c) PCR Genotyping of E2, E6 and E9 heterozygous (het) and deficient (def) mice. d) and e) Enumeration of peripheral blood Mo in WT, E2, E6 and E9 domain-heterozygous (het) and -deficient (def) mice. Parametric t-tests performed relative to WT, ** $p < 0.01$ *** $p < 0.001$. f) FACS gating and representative flow plot for each genotype in d) and e). Please refer to supplementary figure S4.

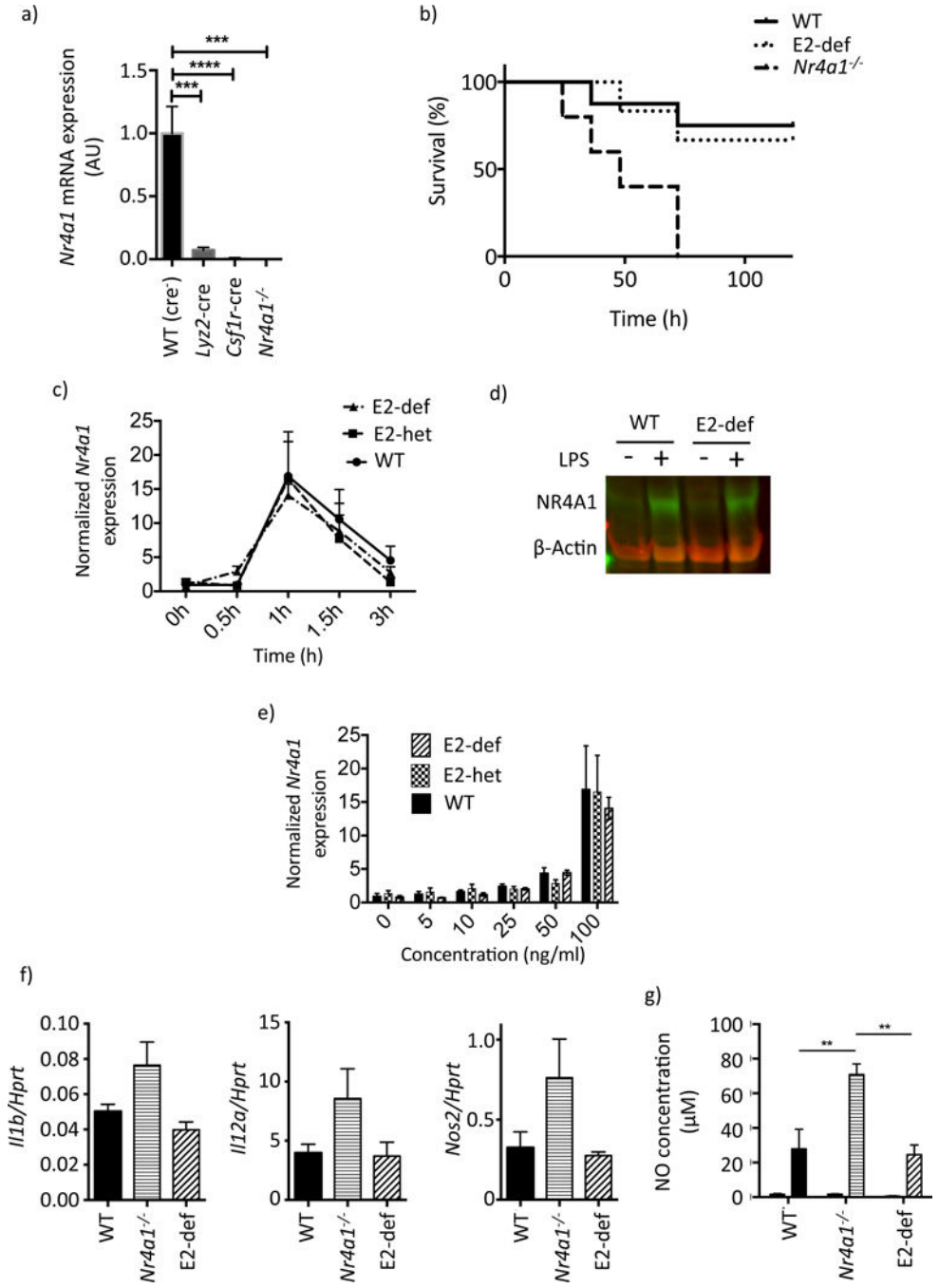

Figure 4. E2 does not regulate *Nr4a1* mRNA expression in response to inflammatory stimuli

a) *Nr4a1* mRNA expression in thioglycollate-elicited macrophages obtained from *Nr4a1*$^{flox/flox}$ mice crossed to *Lyz2-cre* and *Csf1r-cre*, WT (Cre^{-} littermates) are shown as control. b) Kaplan-Mayer curve showing survival of WT, E2 domain-deficient and *Nr4a1*$^{-/-}$ mice in response to a single dose of 2.5mg/kg LPS I.P. Mantel-Cox (Log rank) test results: WT vs. *Nr4a1*$^{-/-}$ p<0.01, E2 domain-deficient vs. *Nr4a1*$^{-/-}$ p<0.05, E2 domain-deficient vs. WT p>0.05. c) RT-PCR time course of *Nr4a1* mRNA in primary thioglycollate-elicited macrophages following LPS stimulation (100ng/ml). d) Immuno blot showing *Nr4a1*

expression 1h post LPS stimulation (100ng/ml). e) *Nr4a1* mRNA expression in dose escalation at 1h post LPS stimulation. f) Inflammatory cytokine mRNA expression in primary peritoneal macrophages 1h post injection of 1ug LPS I.P. g) Nitric oxide in culture supernatant 96h after LPS stimulation.

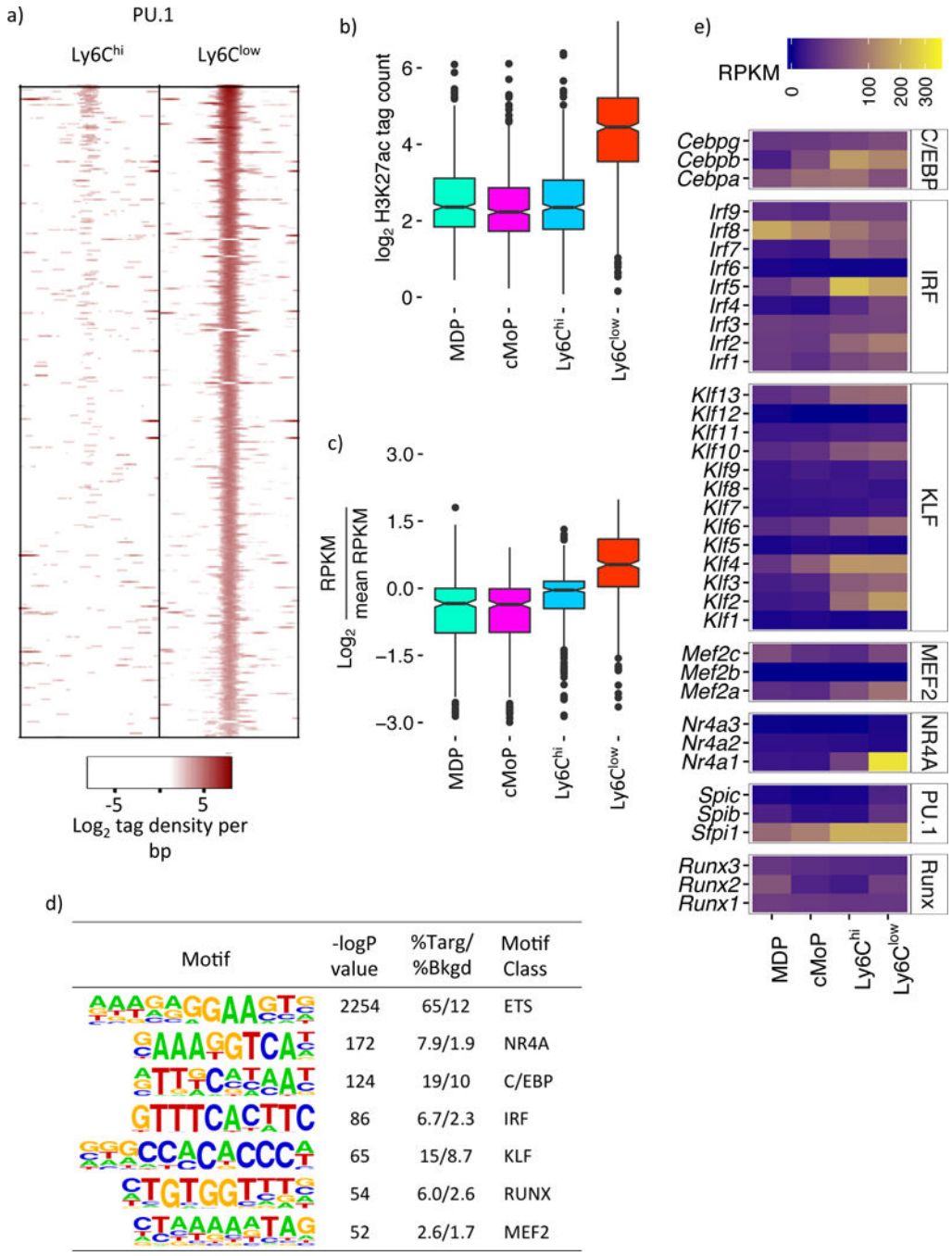

Figure 5. Identification of motifs associated with Ly6C^{low} Mo development

a) Normalized PU.1 ChIP-Seq signal in Ly6C^{hi} and Ly6C^{low} Mo of Ly6C^{low} Mo-specific PU.1 sites ±400 bases from PU.1 peak center. b) H3K27ac ±500 bases of Ly6C^{low} Mo-specific PU.1 peaks. c) Relative expression of genes proximal to Ly6C^{low} Mo-specific PU.1 peaks. d) Overrepresented motifs in Ly6C^{low} Mo specific PU.1 peaks identified by *de novo* enrichment analysis. e) RNA-Seq expression amounts of TFs predicted to bind motifs in d). Please refer to supplementary figure S5a.

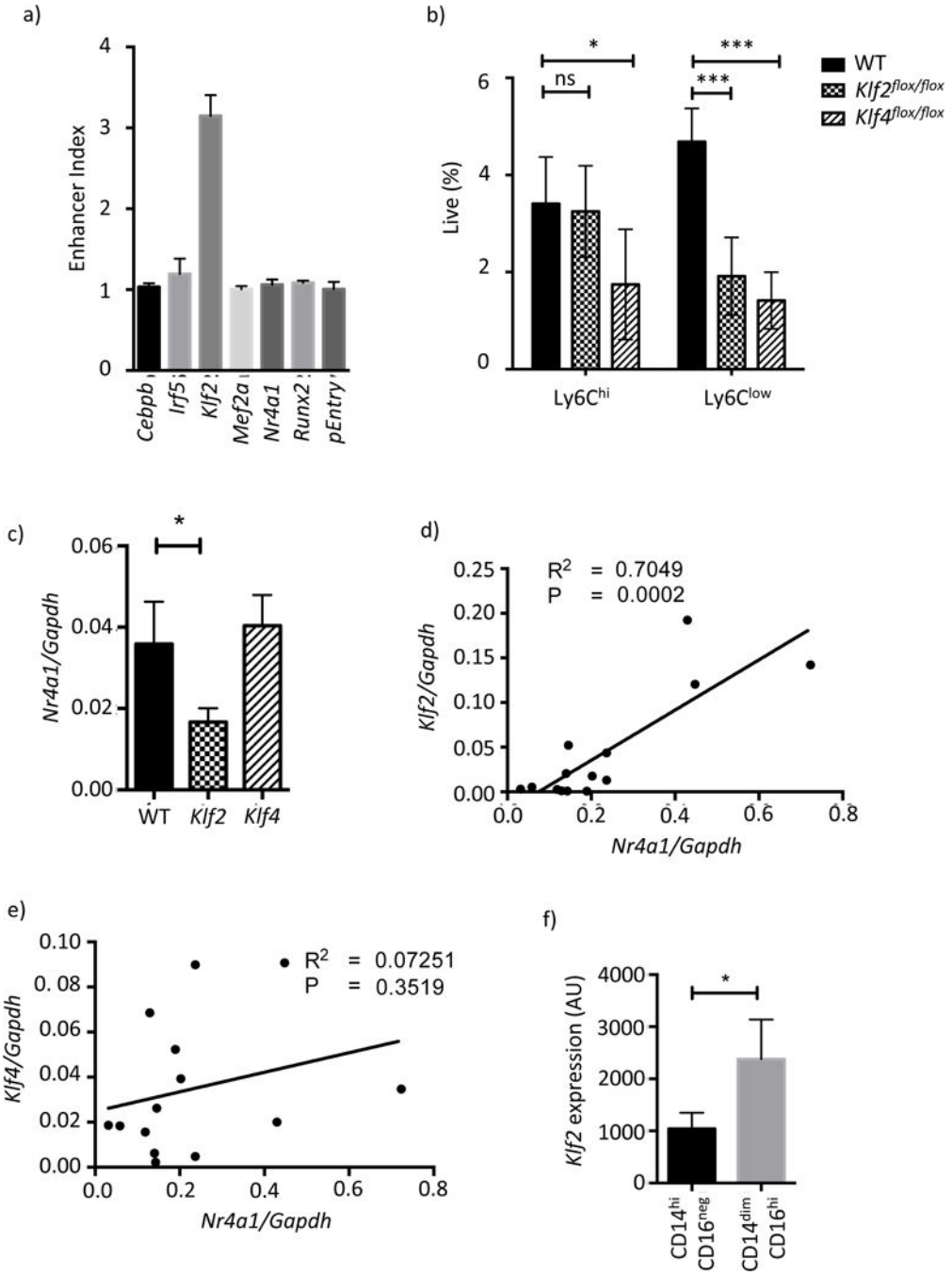

Figure 6. *Klf2* drives Ly6C^{hi} to Ly6C^{low} Mo conversion via E2

a) Overexpression of candidate TFs in the presence of pGL4.*Nr4a1*_E2 and pGL4.*Nr4a1* reporter vectors in RAW264.7 cells. The enhancer index is calculated as described in the methods. b) Blood Mo frequencies in *Lyz2-cre Klf2$^{flox/flox}$* and *Lyz2-cre Klf4$^{flox/flox}$* mice. c) *Nr4a1* mRNA expression amounts in primary Ly6C^{hi} Mo d) *Klf2* mRNA correlated against *Nr4a1* in Ly6C^{low} Mo e) the same data as d) for *Klf4* mRNA. f) *Klf2* mRNA expression amounts in primary human Mo subsets as measured by microarray. Please refer to supplementary figures S5b and S6.

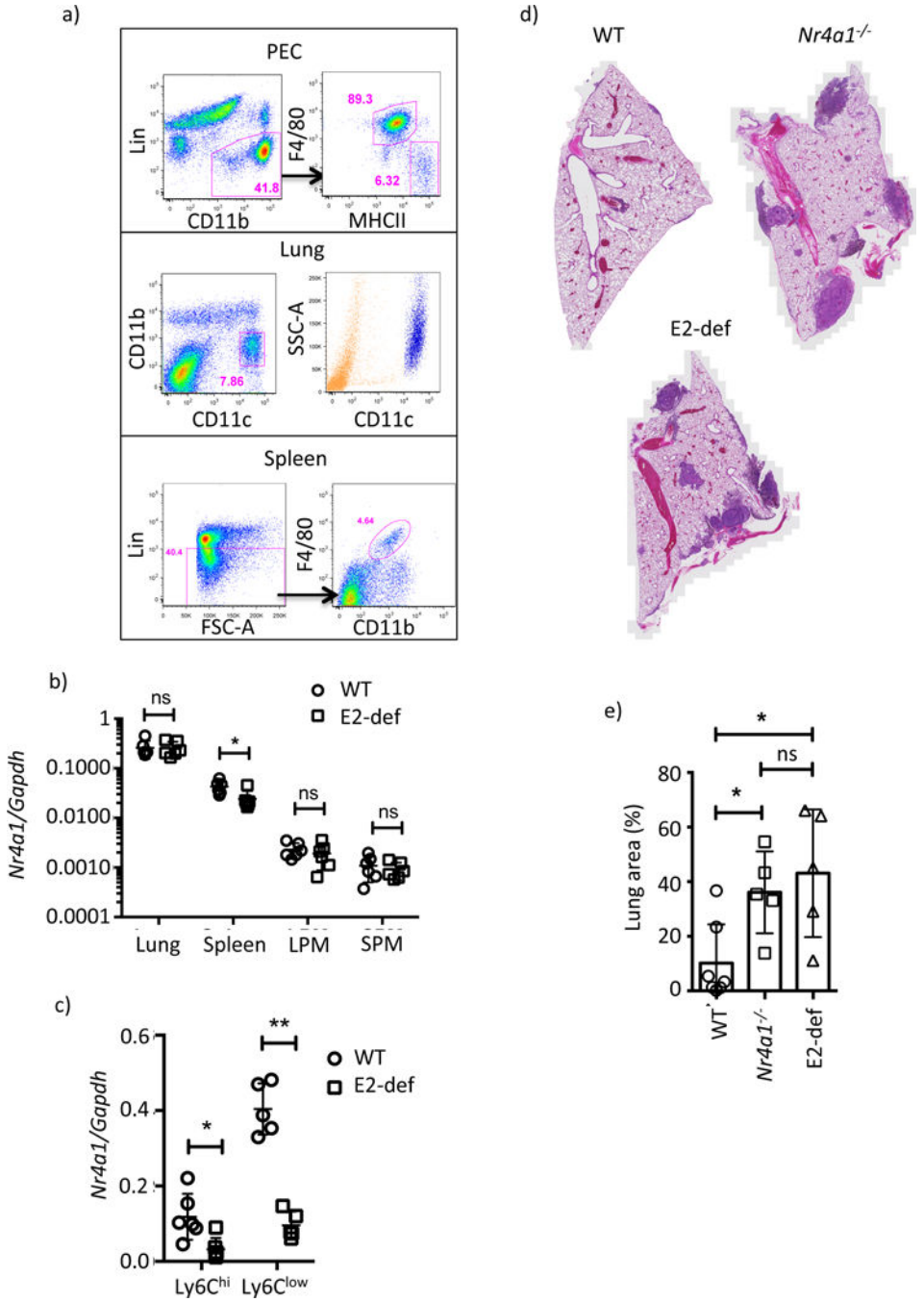

Figure 7. E2 is a monocyte-specific enhancer

a) Gating scheme for tissue macrophage sorting. All cells were previously gated on live singlets. The side scatter high profile of lung CD11c^{+} macrophages is shown in the right panel (blue). b and c) Relative *Nr4a1* mRNA expression in tissue macrophages and blood Ly6C^{hi} and Ly6C^{low} Mo. Statistics for b) and c) measured by students t-test * $p<0.05$, ** $p<0.01$. d) Representative sections of B16F10 tumors in WT, *Nr4a1*$^{-/-}$ and E2 domain-

deficient mice. e) and f) Quantification of cancer metastasis area, error bars represent SD statistics were analyzed by ANOVA * $p<0.05$. Please refer to supplementary figure S7.